J. Membrane Biol. 8, 259 – 301 (1972)

The Route of Passive Ion Movement through the Epithelium of *Necturus* Gallbladder

E. Frömter

Dept. of Physiology, University of California, Medical Center, Los Angeles, California 90024 and Max-Planck-Institut für Biophysik, 6 Frankfurt am Main 70, Kennedyallee 70, Germany

Received 28 September 1971

Summary. Electrophysiological experiments were performed on *Necturus* gallbladder to determine whether the main route of passive ion flow was via the cells or via a paracellular shunt path. In the first approach the following values were determined: the transepithelial resistance, the ratio of the voltage deflections across the luminal and basal cell membrane during transepithelial current flow, and the voltage spread within the epithelial cell layer during intracellular application of current pulses. From these data the luminal and basal cell membrane resistances were calculated to be 4,500 and 2,900 Ωcm^2, respectively, whereas the transepithelial resistance was only 310 Ωcm^2, indicating that approximately 96% of the transepithelial current bypassed the cells. This result was confirmed in a second approach, in which the intracellular voltage deflections were found to remain approximately constant, when the current pulses were passed from a cell into the interstitial compartment with the luminal compartment being empty or when they were passed from the cell into both external compartments simultaneously. In the third approach current was passed through the epithelium and a voltage-scanning microelectrode was moved across the surface of the epithelium to explore the induced electrical field. Significant distortions of the field were observed in the immediate vicinity of the cell borders. This result indicated that the paracellular shunt, which carries the main part of the transepithelial current, leads through the terminal bars and that the terminal bars or "tight" junctions are *not* tight for transepithelial movement of small ions in gallbladder epithelium.

Epithelia are sheets of cuboidal cells which are held together by small junctional complexes, named "Schlußleisten" or terminal bars. Since the discovery of the terminal bars at the end of the last century, there has been much speculation as to whether they are tight or whether they permit exchange of matter between the two compartments which the epithelium separates. As evidenced by the commonly used term "tight junction", the most widely accepted view was that the terminal bars were tight. This view was supported, for example, by electron-microscopic studies which

demonstrated that the junctions were impermeable to large molecules like hemoglobin [17], ferritin [29, 38] and colloidal lanthanum [22]. Recently, however, a number of interesting observations has been made which suggest that in some epithelia the terminal bars might be permeable to small ions.

The first tentative evidence was obtained by Lundberg [27] in cat sublingual gland and by Ussing and Windhager [41] in frog skin. Later, Windhager, Boulpaep and Giebisch [44], Hoshi and Sakai [23] and Boulpaep [8] showed that in *Necturus* and *Newt* kidney the conductance of the proximal tubular epithelium was higher than the conductance of the peritubular cell wall alone. This and other observations pointed to the existence of a high conductance paracellular shunt path. The same conclusion was reached for the proximal tubular epithelium of the rat kidney by Frömter, Müller and Wick [20] from a comparison of the overall permeability properties of the epithelium with the permeability properties of the peritubular cell membrane. Similarly, Barry, Diamond and Wright [5] found that the permeability and conductance properties of the gallbladder epithelium were largely different from the properties of cell membranes in general and concluded from these and other observations that the passive ion permeation through the gallbladder occurred predominantly via high conductance shunts. Further evidence for the existence of a paracellular shunt was presented by Clarkson [10] in rat intestine, and by Blum, Hirschowitz, Helander and Sachs [7] in *Necturus* gastric mucosa, and Bentzel, Parsa and Hare [6] discussed that a significant amount of the transepithelial water flux in *Necturus* proximal tubules might bypass the cells.

Despite this mostly indirect evidence for the existence of a shunt path it still remained a matter of speculation, whether the shunt could be identified with the terminal bars or whether it was located elsewhere. As alternative possibilities, physiological or traumatic cell desquamations had been discussed, and in epithelia which consist of different cell types, such as *Necturus* kidney tubules, gastric mucosa and intestine, a particular cell type could have been involved. Another point which remained uncertain was the exact magnitude of the shunt conductance compared to the cellular conductance. The only tissues in which calculations have been attempted until now are the renal tubules [8, 44] and the gastric mucosa [7] of *Necturus*. These tissues have complicated geometric structures and different cell types which make an exact evaluation of the data difficult. The uncertainty arises mostly from the fact that the individual cell membrane resistances have to be worked out from an analysis of current spread within the epithelial cell layer, since epithelial cells are electrically coupled [24], and that an

exact mathematical solution of this problem for the tubular geometry is not available. Application of the so-called two-dimensional cable theory to the data may lead to qualitatively correct results but the error involved is difficult to assess.

In view of these difficulties with experiments on kidney tubules we have tried to investigate the problem of the shunt path on the gallbladder which has a much simpler structure. The gallbladder of *Necturus* was chosen. It has a typical, single-layered, flat sheet epithelium without villi, folds or crypts. As verified by light microscopy, the epithelium consists only of one type of uniform cells. The cell diameter is approximately four times larger than that of rabbit gallbladder epithelium. Hence single cells can be viewed through the stereomicroscope and can be impaled with microelectrodes easily.

In the experiments, three different approaches were used to determine the magnitude of the paracellular shunt conductance and to specify its location. They consisted essentially of microelectrode experiments in which potential profiles in response to applied currents were measured within the cell layer or within the immediate vicinity of the luminal epithelial surface of the cells. The technical and theoretical principles of these approaches are described on pages 261 through 268 and in the Appendix. The experiments showed that in *Necturus* gallbladder the conductance of the paracellular shunt path is approximately 24 times higher than the conductance via the cells and that the high conductance shunt is located in the terminal bars.

Theoretical Considerations

The aim of the present study was: 1) to determine whether current flow through the gallbladder epithelium is uniform or whether there are discrete high conductance pathways by which ions can bypass the cells; 2) to determine the conductance of these pathways quantitatively and to estimate which part of the total transepithelial current flows through the shunt path and which part flows through the cells; and 3) to determine the location of the shunt paths.

Appropriate electrophysiological measurements to investigate these problems can be derived from a consideration of the histological structure of the epithelium (Fig. 1). It consists of one layer of uniform cells, which are held together at their luminal ends through the terminal bars *E*. Each cell has one membrane *D* facing the luminal or mucosal fluid compartment and one membrane facing the interstitial or serosal fluid compartment.

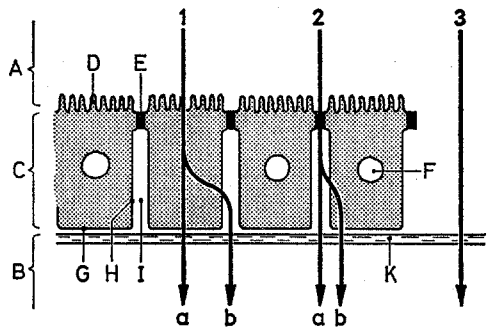

Fig. 1. Schematic representation of a cross section through gallbladder epithelium. *A*, luminal fluid compartment; *B*, interstitial fluid compartment; *C*, cell; *D*, luminal cell membrane with microvilli; *E*, terminal bar; *F*, nucleus; *G* and *H*, basal and lateral part of the basal cell membrane; *I*, lateral intercellular space; *K*, basement membrane. The numbers 1*a* and *b*, 2*a* and *b* and 3 indicate three hypothetical routes for current flow from lumen to interstitium. (For details *see* text)

The latter membrane can be subdivided into two parts: the lateral part, which lines the lateral intercellular space *H* and the basal part which touches the basement membrane *G*. In such an epithelium the following possible routes can be considered for current flow from lumen to interstitium: 1) via the luminal membrane into the cell and from the cell either across the basal part of the cell membrane into the interstitium (1*a*) or across the lateral membrane and the lateral intercellular space into the interstitium (1*b*); 2) through the terminal bars and either along the lateral intercellular space into the interstitium (2*a*) or across the lateral membrane into the cell compartment and across the basal part of the cell membrane into the interstitium (2*b*); 3) along other unspecified paracellular routes (for example, gaps of desquamated cells).

Taking all three possible routes for current flow together, the histological structure of the epithelium can be translated into an electrical equivalent circuit as shown in Fig. 2*a*. Although this circuit may be a fairly accurate representation of the epithelium, it cannot be analyzed directly since only the points *A*, *B* and *C* are accessible to voltage and current electrodes. Measurements between these three points can only yield three lumped resistances as depicted in the equivalent circuit of Fig. 2*b*. To determine the magnitude of the individual resistors of Fig. 2*a* additional information will be required.

The resistors of Fig. 2*b* have been named R_m, R_b and R_s. R_m represents the resistance of the luminal cell membrane. Its meaning is identical in Fig. 2*a* and *b*. R_b can be interpreted as the lumped resistance of the lateral

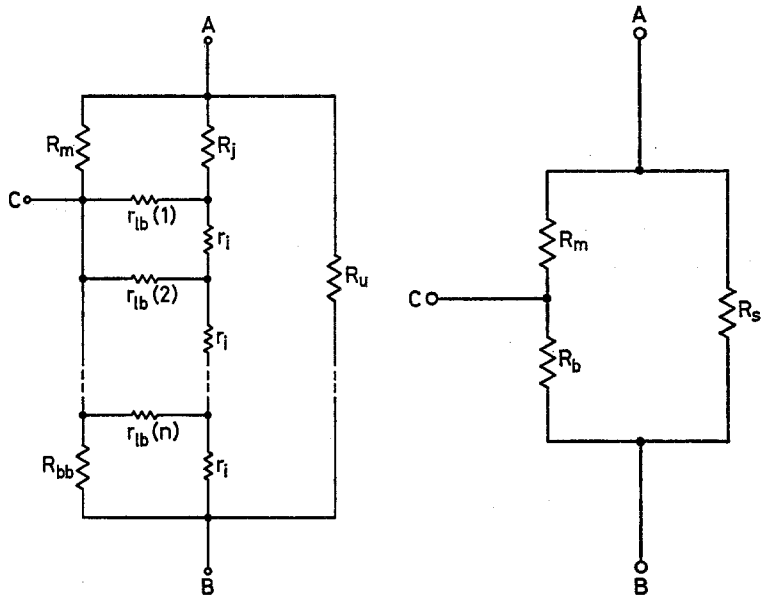

Fig. 2*a* and *b*. Equivalent circuit of an epithelial cell and its share of the paracellular shunt path. *A:* distributed form, comprising the essential elements of Fig. 1; *B:* lumped form, representing the lumped resistors which can be determined in the experiment. R_m and R_{bb} denote the resistances of the luminal cell membrane and of the basal part of the basal cell membrane, respectively. R_j and R_u are the resistances of the junctional complex and of an unspecified shunt path. The resistances of the lateral intercellular space r_i and of the lateral part of the basal cell membrane r_{lb} form a cable-like element which is thought to consist of n subunits. *A*, *B* and *C* are the luminal, interstitial and cellular fluid compartment, respectively, into which electrodes may be placed. The resistivity of the intracellular fluid and of the luminal and interstitial fluid has been neglected. The experiments revealed that R_u was infinite in *Necturus* gallbladder epithelium (*see* below). The meaning of the resistors of Fig. 2*b* is discussed in the text. Both circuits represent a single cell and can only be used to describe measurements on the gallbladder if the voltage response of all neighboring cells is identical. This requirement is fullfilled in the measurements with transepithelial current flow and it is also partially fulfilled in experiments with current injection into single cells because the current spreads horizontally within the cell layer (for a detailed discussion of the problem *see* Appendix, pp. 294 through 296). In the absence of current spread, determination of R_z would require the consideration of an additional resistor parallel to R_s in Fig. 2*b* to account for the shunting effect of the other cells and their shunt paths

and basal part of the basal cell membrane. Since the resistivity of biological membrane material is always several orders of magnitude higher than the resistivity of biological fluids and since the space width in gallbladder epithelium is in the order of 1 μm under control conditions [39] we can assume as a first approximation that r_i is negligible compared to r_{lb} and that

$n \cdot r_i$ is also negligible compared to R_{bb}. This assumption leads to

$$\frac{1}{R_b} \sim \frac{1}{R_{bb}} + \frac{n}{r_{lb}}. \tag{1}$$

R_s, finally, is the lumped resistance for the transepithelial current which may bypass the cells. It may either flow across R_j and along the chain of resistor r_i or along an unspecified path R_u.

To determine the values of R_m, R_b and R_s, three independent measurements are required. From a variety of different possibilities the following two combinations of each three measurements were chosen, which will be named Method I and Method II.

Method I

Experiment 1: Determination of the Specific Transepithelial Resistance R_t. In the first experiment of this method, current is passed from the luminal A to the interstitial fluid compartment B and the transepithelial voltage drop is recorded between A and B with a separate pair of electrodes. From these data the specific resistance of the epithelium for transepithelial current can be calculated. It is conveniently expressed per cm^2 of epithelial surface. From Kirchhoff's law:

$$\frac{1}{R_t} = \frac{1}{R_s} + \frac{1}{R_m + R_b}. \tag{2}$$

Experiment 2: Determination of the Voltage Divider Ratio $\Delta V_m / \Delta V_b$. In this experiment current is passed from lumen A to interstitium B and, by means of an intracellular microelectrode, the voltage drop ΔV_m is measured across the luminal membrane (between C and A) and the voltage drop ΔV_b is measured across the basal membrane (between C and B). The ratio of both voltages is equal to the ratio of the resistances R_m to R_b.

$$\frac{\Delta V_m}{\Delta V_b} = \frac{R_m}{R_b} \equiv a. \tag{3}$$

Experiment 3: Determination of the Specific Resistance R_z *for current Flow from the Cellular Compartment into the External Fluid Compartments.* In this experiment, current is passed from the cellular compartment C into both [1] external fluid compartments A and B and *ideally* the voltage drop

1 Experimentally it was found that the results did not differ when the indifferent current electrode was placed into either one external fluid compartment or into both external fluid compartments simultaneously (*see* p. 284 and for explanation *see* Appendix, pp. 295–296).

between C and A or B is measured. Since current can flow via R_m into A and via R_b into B, we obtain

$$\frac{1}{R_z}=\frac{1}{R_m}+\frac{1}{R_b}. \tag{4}$$

In reality, however, the determination of R_z is more complicated. From the work of Loewenstein and co-workers [24–26], it can be predicted that the cells of gallbladder epithelium like those of other epithelia are electrically coupled by low resistance cell-to-cell junctions. Consequently we expect that current, which is injected into one cell by means of a microelectrode, does not leave the cell via the luminal and basal membrane alone but flows also into neighboring cells. In this case it is no longer possible to derive R_z from the current-induced voltage drop ΔV_m across the luminal membrane of the current cell. Instead, the voltage spread in the epithelial cell layer has to be investigated and ΔV_m has to be determined as a function of radial distance x from the current cell. A mathematical analysis of this problem and an appropriate way to derive R_z from such data is given in the Appendix. R_z as well as R_t can be expressed per cm^2 of epithelial surface. In both cases the latter possibility was chosen.

When R_t, $\Delta V_m/\Delta V_b$ and R_z are known, the resistances of the luminal cell membrane R_m, of the basal cell membrane R_b, and of the shunt path R_s can be calculated. Combining Eqs. (2) through (4), leads to:

$$R_m=(1+a)\,R_z, \tag{5}$$

$$R_b=\frac{(1+a)}{a}\,R_z, \tag{6}$$

$$R_s=\frac{(1+a)^2\,R_t\,R_z}{(1+a)^2\,R_z-aR_t} \tag{7}$$

and the ratio of the shunt conductance to the cellular conductance is

$$\frac{R_m+R_b}{R_s}=\frac{(1+a)^2\,R_z-aR_t}{aR_t}. \tag{8}$$

Since R_t and R_z will be expressed in relation to 1 cm^2 of epithelial surface the dimensions of R_m, R_b and R_s will also be $\Omega\ cm^2$.

Method II

Another possible choice of measurements is:

Experiment 1: Determination of the voltage divider ratio $\Delta V_m/\Delta V_b$, as described under Method I.

Experiment 2: Determination of the specific resistance R_z for current flow from the cellular compartment into the external fluid compartments as described under Method I.

Experiment 3: Determination of the specific resistance R for current flow from the cellular compartment C *into the interstitial compartment* B *with the luminal compartment* A *being empty.* This resistance will be named R_z'. Fig. 2*b* yields:

$$\frac{1}{R_z'}=\frac{1}{R_b}+\frac{1}{R_m+R_s}. \tag{9}$$

Strictly speaking, this equation would require that current is passed into all cells simultaneously. Since we are dealing with an electrically coupled epithelium however, Eq. (9) can still be used if the shunting effect of the epithelium surrounding the current cell is reduced. This can be achieved by emptying the luminal fluid compartment as discussed in the Appendix, p. 296.

From these three measurements, R_m and R_b can be calculated according to Eqs. (5) and (6), and R_s according to

$$R_s=\frac{(1+a)^2 R_z(R_z'-R_z)}{R_z+a(R_z-R_z')}. \tag{10}$$

However, since determination of R_s is essentially based on the difference between R_z and R_z', and since both values, R_z and R_z' must be determined by curve-fitting procedures, we can anticipate that the result will be less conclusive quantitatively than the result of Method I. Hence, instead of calculating R_s it would seem more appropriate to use these measurements only as a qualitative test for the existence of a paracellular shunt. This can be done as follows. By dividing Eqs. (4) through (9) the following simple relation is obtained:

$$\frac{R_z'}{R_z}=1+\frac{R_b R_s}{R_m^2+R_m R_s+R_m R_b} \tag{11}$$

which can be further simplified by use of Eq. (3) to

$$\frac{R_z'}{R_z}=1+\frac{R_s}{a(R_m+R_b+R_s)}. \tag{12}$$

This equation allows the following conclusions to be drawn from the experiments:

1) If $R_s \ll R_m$ and R_b the ratio R_z'/R_z should approach unity. Hence, this result would indicate the presence of a highly conducting paracellular shunt. Furthermore, if in addition $R_m \sim R_b$, it can be seen that the ratio R_z'/R_z

immediately yields the relative magnitude of the shunt resistance *vs.* the resistance of the cellular transport route.

$$\frac{R_z'}{R_z} \sim 1 + \frac{R_s}{R_m + R_b}. \tag{13}$$

2) On the other hand, if the resistance of the paracellular shunt is comparable to or greater than R_m and R_b, the ratio R_z'/R_z should be greater than 1. If R_s approaches infinity the second term in the right-hand side of Eq. (9) vanishes and we obtain

$$\frac{R_z'}{R_z} = 1 + \frac{R_b}{R_m} = 1 + \frac{1}{a}. \tag{14}$$

The application of Methods I and II to the gallbladder epithelium should allow us to prove or disprove the existence of a paracellular shunt path and to calculate the magnitude of the resistors R_m, R_b and R_s (compare Fig. 2*b*). In case of a significant shunt conductance the next step of the analysis will be to interpret the lumped resistors R_b and R_s in terms of the histological structure of the epithelium, that is, in terms of the individual resistors of the equivalent circuit depicted in Fig. 2*a*.

To distinguish whether the shunt current flows through the terminal bars (via R_j in Fig. 2*a*) or through other unspecified channels (via R_u in Fig. 2*a*), advantage can be taken of the fact that the solutions in compartment *A* (and *B*) act as volume conductors of finite conductivity. If the major part of the transepithelial current is funneled through discrete areas of high conductance the current lines should concentrate in the immediately adjacent region of the volume conductor, as illustrated in Fig. 3*a*, and the equipotential planes should become distorted. If we now move a *voltage-scanning* electrode through this region at a fixed distance from and parallel to the epithelial surface (for example, along line *H* in Fig. 3*a*) and record the potential against a second electrode of fixed position in the same fluid compartment, we should be able to detect inhomogeneities of the electrical field (provided that the current density and the resistivity of the solution in the fluid compartment are high enough to yield measurable differences). If, in addition, the movement of the electrode can be observed under the microscope, it should be possible to correlate the results of the voltage scan with the structure of the epithelium and to specify the anatomical location of shunts.

To determine whether the resistance of the lateral intercellular spaces contributes a significant amount to R_b and R_s ideally the potential profile along the spaces should be measured. Since this was not feasible, however,

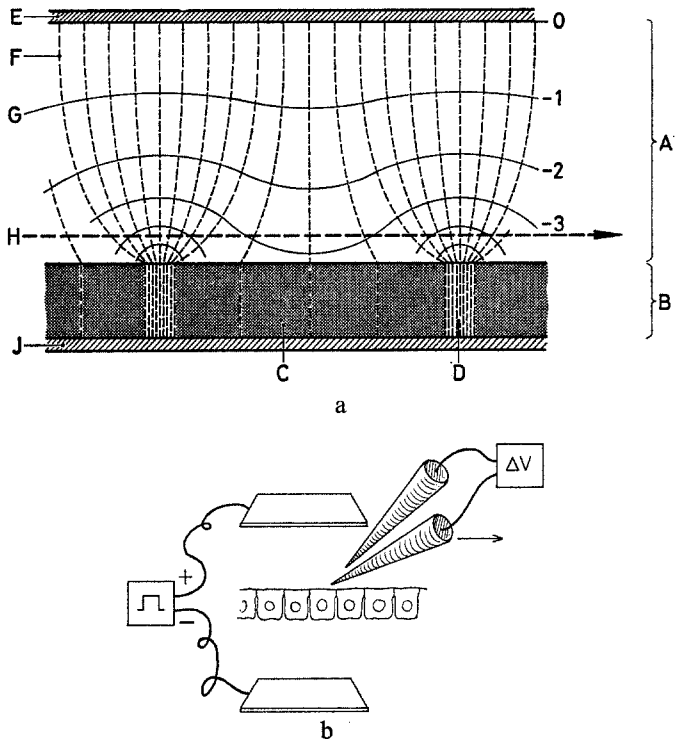

Fig. 3*a* and *b*. Principle of the voltage scan experiments. *A:* Distribution of current flow in the vicinity of a shunt path. *B:* Experimental set up (*see* p. 272). *A*, volume conductor; *B*, membrane; *C*, region of low membrane conductance; *D*, region of high membrane conductance; *E*, positive current electrode; *F* current line; *G*, equipotential line; *H*, proposed path for the movement of a voltage scanning electrode; *J*, negative current electrode. During flow of inward current (volume conductor positive, membrane negative) the voltage scanning electrode should record a more negative potential over a region of high membrane conductance than over a region of low membrane conductance

an attempt will be made to estimate the magnitude of this resistance from the dimensions of the spaces. This is possible since the resistivity of the fluid within the lateral spaces cannot be vastly different from the resistivity of interstitial fluid in general.

Experimental Techniques

Necturi were obtained from Lemberger Co., Oshkosh, Wisconsin. The animals were kept for up to 3 weeks at 15 °C in aerated water tanks. They were fed with goldfish. To remove the gallbladder, animals were either anaesthetized with MS 220 (Sandoz) or decapitated. After dissection, the gallbladders were emptied and care was taken that no bile contaminated

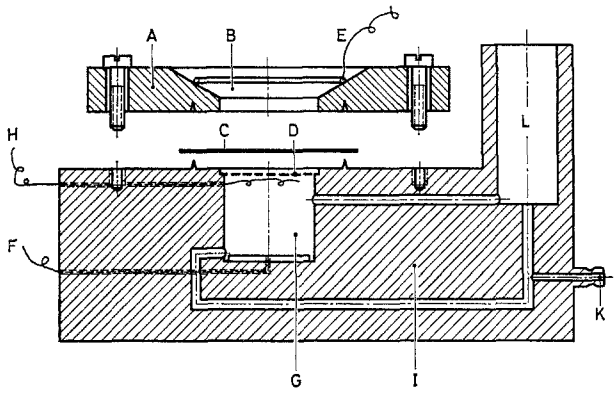

Fig. 4. Cross section of the chamber used for mounting the gallbladders. *A*, upper half-chamber; *B*, luminal fluid compartment; *C*, gallbladder; *D*, supporting grid; *E* and *F*, Ag-AgCl electrodes for passing current transepithelially; *G*, interstitial fluid compartment; *H*, Ag-AgCl electrode for connecting the circuit to ground; *I*, lower half-chamber. The fluid in the lower half-chamber could be circulated and oxygenated by a bubble lift, which was operated through nozzle *K*, whereas the fluid in the upper compartment was frequently replaced. The hydrostatic pressure difference across the gallbladder was usually kept at zero. It could be changed by adjusting the fluid level *L*. Instead of the ring-shaped electrode *E* in some experiments a star-shaped electrode was used, which had the same overall width as the exposed surface of the gallbladder and was thought to distribute the current more uniformly. However, no difference in the results was observed

the serosal surface. The empty bladders were opened by a longitudinal section and then mounted as a flat sheet in a modified Ussing chamber (Fig. 4) which allowed free access to the mucosal surface of the tissue. During mounting, moderate stretch was applied to prevent folding of the epithelium. The exposed surface was 0.6 cm^2.

With very few exceptions, which are specified later, the bathing fluids on both sides of the gallbladder were always identical and consisted of Ringer's solution containing 115.4 Na^+, 3 K^+, 2.7 Ca^{++}, 118.7 Cl^- and 2.4 HCO_3^- (all concentrations in mEquiv/liter). The pH was ~7.4. In some experiments, the luminal fluid compartment was emptied by sucking off the fluid. Through the use of molten tip suction pipettes of 20-μm outer diameter the remaining fluid film could be reduced to a thickness of less than approximately 5 μm as judged by immersion of fine glass rods. All experiments were performed at room temperature of 22 to 25 °C.

Microelectrodes and Micropuncture Techniques

All intracellular impalements were done with Ling-Gerard micropipettes, filled with 2.7 M KCl solution. The pipettes were pulled from

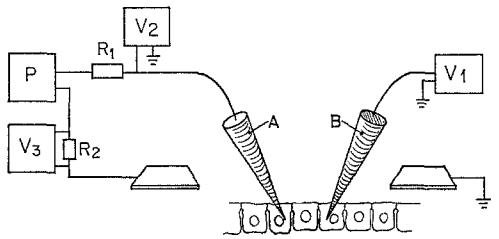

Fig. 5. Experimental set up for determining the voltage spread within the epithelial cell layer. (For details *see* text)

Pyrex glass tubing (Corning) of 1.5 mm OD and 1.0 mm ID in a vertical puller (Narishige). Electrodes with tip potentials >5 mV were discarded. The electrode resistance was usually between 20 and 40 MΩ, but sometimes, when measuring voltages, electrodes with resistances up to 100 MΩ were used. The electrodes used in the voltage scan experiments were filled with Ringer's solution, and their tips were broken to reduce the electrical resistance to values between 10 and 20 MΩ. The outer tip diameter of the latter electrodes was ~ 1.4 μm.

During the experiments, the microelectrodes were mounted in special Lucite holders on micromanipulators (Leitz). All measurements using microelectrodes were done under direct observation through a stereozoom microscope (Bausch and Lomb) at $150\times$ magnification. For measuring distances, an eyepiece micrometer was used. To improve the accuracy in determining the electrode position, small color marks were attached to the electrode shaft at known distances from the tips. The measurements were performed on a heavy table using four Airmounts no. 1 X 84D-1 (Firestone) as shock absorbers.

Electrical Circuit and Instrumentation

The basic electrical circuit, which was used to measure the intraepithelial current spread, is depicted schematically in Fig. 5. Two microelectrodes were used to impale individual epithelial cells. Electrode *A* served to pass current pulses into one cell and was left in place for up to 1 hr while various neighboring cells were punctured with electrode *B* and the current-induced voltage deflections were recorded as a function of interelectrode distance. To ascertain the proper intracellular position of the microelectrode and to avoid artifacts through leaky impalements, the cell potential was measured across the luminal cell membrane with electrometers V_1 (Keithley, model

604) and V_2 (Keithley, model 610B)[2] and continuously recorded on a 3-channel pen recorder (Rikadenki). In contrast to rabbit and fish gallbladder [5, 13, 47], the gallbladder of *Necturus* generates a small transepithelial potential difference, when it is exposed to Ringer's solution on either side. The mean value of eight observations was 2.5 ± 3.1 mV, lumen negative. Hence, it follows that the potential difference across the basal cell membrane must have been slightly higher than that measured across the luminal cell membrane. Square wave current pulses were passed through electrode A from a stimulus isolation unit P (W.P. Instruments, model PC 1) which was driven by a modified Grass stimulator (model SD 5). The current source was virtually ground free (isolation resistance $\sim 10^{12}$ Ω). To reduce the d-c current offset from the stimulus isolator to negligible values it had to be operated on the constant voltage mode. Resistor R_1 ($\sim 2 \times 10^9$ Ω) served to convert the pulses into approximately constant current pulses. The current could be measured as the voltage drop across R_2 (10^4 Ω) with the differential electrometer V_3 (Transidyne model MPA 6). Small current changes caused by polarization of microelectrode A could also be detected by monitoring the potential across microelectrode A with electrometer V_2 during the pulse. The current drain through resistor R_1 from the cell was negligible. It should cause a depolarization of ~ 30 μV as can be calculated from the input resistance of the cells.

With microelectrodes of 30 MΩ resistance, the rise time (0 to 100%) of a square wave current pulse through electrode A was of the order of 2 msec, and the rise time of a voltage signal in circuit B was 1 msec. In most experiments, a pulse duration of 1.2 sec was used. To reduce disturbances to a minimum, usually only one current pulse was applied through electrode A for every cell punctured with microelectrode B. The voltage response V_1 and the voltages V_2 or V_3 or both were displayed on an oscilloscope (Tektronix, model 565) and photographed. Instead of V_3, in most cases we preferred a double tracing of V_2 at high sensitivity to monitor the membrane potential of the current cell immediately before and after the current pulse, and at low sensitivity to monitor the resistance of the current microelectrode during the pulse. The smallest voltage deflection which could be measured accurately with microelectrode B was ~ 400 μV. This limit was mainly determined by fluctuations of the cell membrane potential.

For determination of the transepithelial resistance and of the voltage divider ratio, current was passed transepithelially through electrodes E

2 For proper determination of the membrane potential with V_2, the resistor R_1 was disconnected.

and F (in Fig. 4), and the microelectrodes were used to determine the voltage steps across the epithelium. R_1 was disconnected and microelectrode A was left in the upper fluid compartment immediately adjacent to the epithelial surface to monitor the potential difference against electrode H (Fig. 4) while electrode B was advanced into the epithelium and measured the current-induced voltage deflections in the cell interior and, after further advance, in the subepithelial connective tissue. Sudden appearance or disappearance of a cell potential during the advance was taken to indicate the proper electrode position. The current pulses were obtained from a separate current source (Devices stimulator Mark IV) which was also driven by the Grass SD 5 stimulator. Duration of the current pulse was usually 100 msec and current density was ~ 50 μamps/cm^2. Since the gallbladder epithelium exhibits already marked polarization effects at these current densities (*see* below), only the instantaneous voltage deflections were worked out from the photographs (at 18 msec after onset of current).

In the voltage scan experiments current pulses of up to 2.8 mamps/cm^2 and 1.2-sec duration were passed through the epithelium as described above. The frequency was 0.2 sec^{-1}. To search for inhomogeneities of the electrical field in the neighborhood of the terminal bars, two identical microelectrodes were connected to the inputs of the differential electrometer (Keithley, model 604) (compare Fig. 3*b*). One microelectrode was kept at constant position in the fluid bath, while the other electrode was moved slowly in small intervals across the mucosal surface of the epithelium. The potential difference was recorded continuously on the pen recorder and whenever the electrode tip passed over a cell border, a mark was made. To avoid changes in tip potentials when the electrode touched the cell surface, the electrodes were filled with Ringer's solution.

Analysis of Data

In the experiments on intraepithelial current spread, electrode A was left in the current cell until the voltage deflections had been measured in at least 10 different cells with electrode B. Measurements in which the membrane potential of either the current cell or the voltage cell had dropped to values below 40 to 45 mV, or measurements in which the resistance of electrode A had risen to values above 70 MΩ during the current pulse, were terminated and the data were discarded.

For determination of the constants A and λ (compare Appendix) from the measurements, the method of Shiba [34] was used. The data from individual experiments were plotted as log ΔV against distance on transparent

paper and compared to a set of Bessel functions $Y=K_0\left(\frac{x}{\lambda}\right)$ which had been calculated for nine different values of λ ranging from 240 to 750 μm. The best fitting curve was selected by simple inspection (compare Fig. 12). The vertical displacement of the papers required to adjust the experimental points to this curve yielded the value of constant A. In connection with mean values standard deviations (SD) are given throughout the paper.

Results

The Cell Membrane Potential

Despite the fact that the cells of *Necturus* gallbladder are comparatively large, the measurements of the cell membrane potentials presented some unexpected problems with regular or irregular fluctuations, variations among individual animals and probably seasonal variations. Among a total of approximately 1,200 impalements, not a single puncture was observed in which the potential would suddenly jump to a negative value and then remain constant without wriggles or creeps as we have seen for example in frog skeletal muscle cells or sometimes even in the tiny cells of rat proximal tubules. Often, following the initial jump, the potential difference increased further for 5 to 10 sec and then declined slowly to reach an almost constant value after about 1 min. Occasionally, however, more complex time courses were observed. Spontaneous fluctuations were frequent. They were mostly irregular and slow and had an amplitude of a few mV but were occasionally greater. In two of 53 gallbladders the cells showed regular synchronous membrane potential oscillations of 14- to 24-mV amplitude. The time course was almost exactly a sine wave with a period of ~6-min duration. These gallbladders were not used for the measurements reported below.

The absolute magnitude of the potential difference was comparable to, but in general a little smaller than, the magnitude of the cell potentials in proximal tubules of *Necturus* [21], *Newt* [33] and rat kidney tubules [43] and considerably smaller than that of frog skeletal muscle [2, 30]. Fig. 6 shows a frequency distribution of 37 cell potentials which were measured in a series of pilot experiments in January, 1971. These potentials were stable within ±2.5 mV for at least 1 min. The peak is between 60 to 65 mV (cell interior negative) and the arithmetic mean would be 59.1 ± 8.9 mV. Further analysis of the distribution showed that the large variation was predominantly a variation in the individual gallbladders, some showing

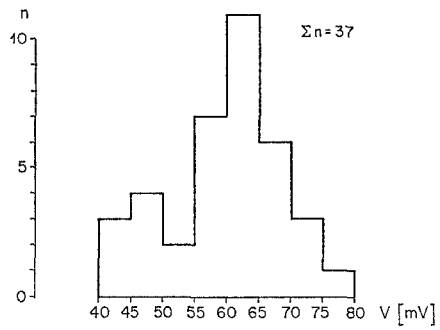

Fig. 6. Frequency distribution of 37 stable cell membrane potentials. *Abscissa:* potential difference in intervals of 5 mV; *Ordinate:* number of observations

only values between 40 and 50 mV, and others, for example, showing only values between 65 and 80. In April and May (1971), when most of the experiments reported below were performed, the cell potentials tended to be lower (compare Table 1 *a*). We are inclined to attribute this to seasonal variations in the conditions of the animals. In a series of pilot experiments we tested the effect of a variety of parameters such as cessation of O_2 supply, increase of bicarbonate in the bathing fluids to 25 mmoles/liter, different mounting conditions, and different length of storage of the animals at 4 or 15 °C. From these parameters, the only one which seemed to have an effect on the cell potential, was excessive stretch during mounting, which led to a slight diminution in potentials.

Determination of the Paracellular Shunt Conductance

Method I

As described above, this method consists of the determination of the following three values: the transepithelial resistance R_t, the voltage divider ratio $\Delta V_m/\Delta V_b$, and the resistance for current flow from the cellular into the external fluid compartments R_z. From these data the shunt conductance $1/R_s$ can be calculated according to Eq. (7).

Application of this concept to a given membrane requires that the resistive elements of the membrane can be treated as simple ohmic resistors. Thus, our first task was to determine whether the resistances R_t and R_z, and the voltage divider ratio, when measured under d-c conditions, were functions of the current density and of the time of current flow. After the time dependence and the linear range of the current-voltage curves had been determined in each case, proper measuring conditions were selected,

and in a final series of six experiments all three values were determined in the same individual gallbladder simultaneously. This protocol was chosen to eliminate variations among individual gallbladders during the calculation of the shunt conductance and thus to improve the reliability of the results.

The Transepithelial Resistance R_t. Under transepithelial current flow the gallbladder epithelium is known to exhibit marked time-dependent polarization effects [42], even though the instantaneous current-voltage relation is linear [46]. Following a square wave current pulse the transepithelial potential difference reached an initial plateau value with a time constant of about 0.7 to 2.7 msec. This value was not constant, however, but decreased or increased slowly, depending on the direction of current flow. Fig. 7*a* shows a typical example of the slow phase potential response of *Necturus* gallbladder during a constant current pulse. The voltage response is asymmetric. During current from mucosa to serosa the potential difference diminishes slowly to reach a plateau after 2 1/2 min whereas during current from serosa to mucosa the voltage rises with time and does not reach a constant level. These effects are functions of the current density. With increasing current densities they are greater and appear faster whereas with decreasing currents they become smaller and eventually disappear at current densities below 5 μamps/cm^2. Although in rabbit gallbladder the voltage creep seems to be caused almost exclusively by the generation of diffusion potentials in unstirred layers [42] this is not so in *Necturus* gallbladder. From observations of the width of the lateral spaces during the polarization process, one can conclude that the voltage creep in *Necturus* gallbladder is mostly caused by opening or closing of the lateral spaces which leads respectively to a decrease or an increase of the transepithelial resistance. A detailed description of these observations will be published separately.

Fig. 7*b* shows a current-voltage diagram which has been obtained from such an experiment. The initial potential readings, plotted as crosses, fall on a straight line, but the values obtained 4 min after onset of current, which are plotted as open circles, show marked deviations. They coincide with the straight line only at low current densities. From this result we conclude that the d-c resistance of the gallbladder is constant and measurable only over a small range of low current densities. Furthermore we conclude that the resistance $(\Delta V/\Delta I)_{I\to 0}$ is identical with the value of the resistance $(\Delta V/\Delta I)_{t\sim 0}$ determined from the instantaneous voltage deflections. This finding is important from a technical point of view, since measurements with higher

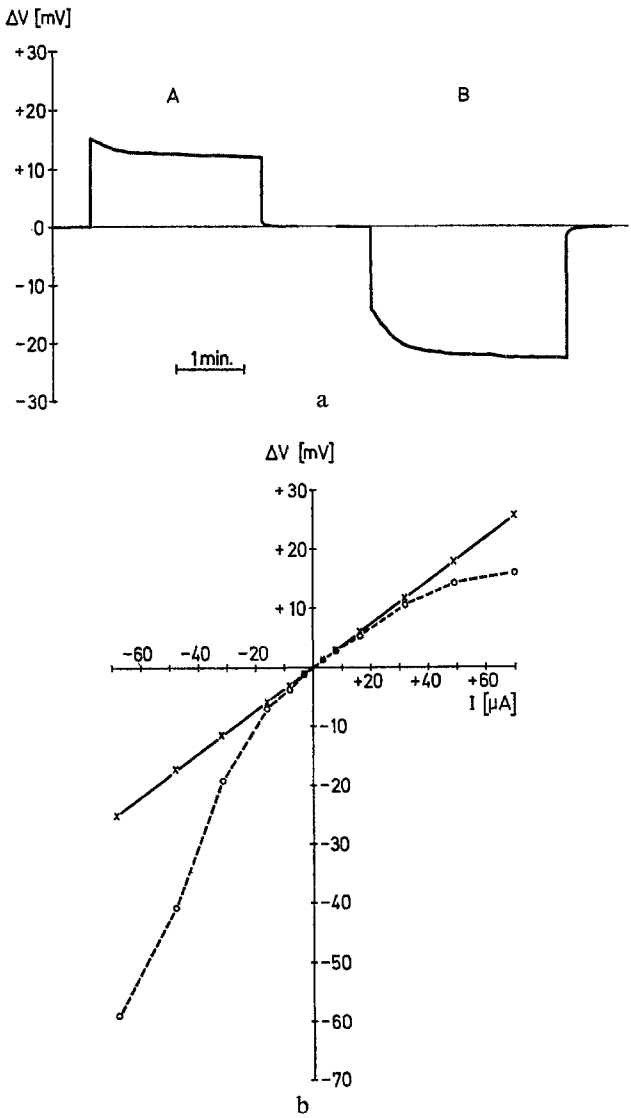

Fig. 7. Current-voltage relation of *Necturus* gallbladder. The upper half shows the transepithelial voltage during flow of constant transepithelial current (31 μamps/cm^2) as a function of time. Current flow was from lumen to interstitium (lumen positive) in *A* and in the opposite direction in *B*. The lower half shows a current-voltage diagram. *Abscissa:* transepithelial current in μamps, current from lumen to interstitium is taken as positive; *Ordinate:* transepithelial potential difference in mV. ×—×—×, instantaneous values, recorded at <0.5 sec after onset of current; ○—○—○, values recorded after 4 min of current flow. After each current pulse of 4-min duration, the gallbladder was allowed to recover during 4 min before the next current pulse of opposite polarity was passed. This protocol required almost 1 hr to finish the experiments. Since in the meantime the control resistance determined at $I \to 0$ was not stable but increased steadily, probably as a consequence of the in vitro conditions, the data were corrected for the increase of the control value

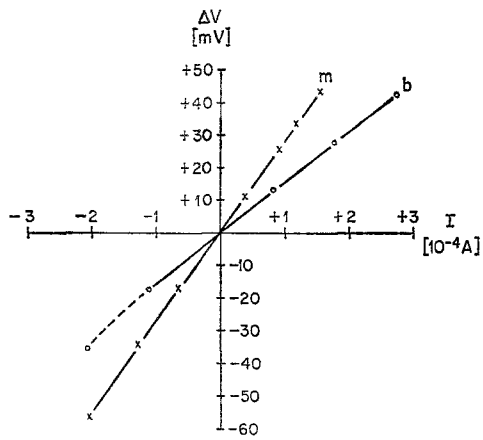

Fig. 8. The voltage deflections across the luminal and basal cell membrane as a function of transepithelial current. *Abscissa:* transepithelial current in 10^{-4} amps, direction of current as in Fig. 7; *Ordinate:* Instantaneous voltage deflections recorded with an intracellular microelectrode across the luminal cell membrane (×—×, *m*) and across the basal cell membrane (∘—∘, *b*). All data were recorded from the same cell

currents at $t \approx 0$ are more accurate than the measurements at low current densities and consequently this method was chosen for the other experiments. From Fig. 7*b* the resistance can be calculated to be 214 Ω cm^2 in this particular gallbladder. The mean value from six other gallbladders (compare Table 1*a*) was 307 Ω cm^2. This value is approximately one order of magnitude greater than the resistance of the rabbit gallbladder [5, 47]. The difference may be due in large part to the different cell dimensions in both epithelia. In contrast to the observations of Barry *et al.* [5], who report that the transepithelial resistance of rabbit gallbladder in vitro declined slowly over hours, the resistances in *Necturus* gallbladder usually increased during the experiment.

The Voltage Divider Ratio $\Delta V_m/\Delta V_b$. During the measurements of the voltage divider ratio the same polarization effects were observed as described above, but the instantaneous current-voltage relation was also linear for both cell sides (Fig. 8). Hence $\Delta V_m/\Delta V_b$ was determined from the instantaneous voltage deflections. In a series of pilot experiments large variations of the voltage divider ratio were observed with mean values ranging from 0.9 ± 0.4 to 3.1 ± 1.2 in individual gallbladders. These variations seemed to exceed the extent which could be attributed to varying properties of the cell membranes themselves and it was thought that the variations might be due to different states of expansion of the lateral spaces. This view was supported by a number of experiments in which the width

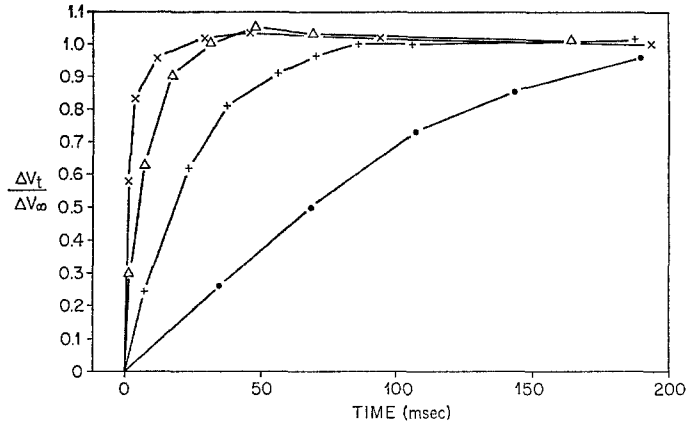

Fig. 9. Time course of the voltage deflections recorded from four different epithelial cells during application of square wave current pulses into a nearby cell. *Abscissa:* time in msec; *Ordinate:* pulse height at time t divided by the constant pulse height before the break of the current after 800 msec (ideally speaking at $t \to \infty$). This type of presentation of the data was chosen because ΔV_∞ varied between 12.4 mV (×—×) and 1 mV (•—•) as a result of the increasing cell-to-cell distance. The distance between the current cell and the voltage cell was 74 μm (×—×), 165 μm (▵—▵), 400 μm (+—+), and 990 μm (•—•)

of the lateral spaces was varied by generating water fluxes across the epithelium through the addition of sucrose (0.5 M) to the luminal or serosal bathing fluid, as described by Smulders, Tormey and Wright [36]. During water flux from mucosa to serosa, which opens the lateral spaces and decreases the transepithelial resistance, the ratio $\Delta V_m/\Delta V_b$ rose from 2.3 to 3.6 or remained constant, and during water flux in the opposite direction, which closes the lateral spaces and increases the transepithelial resistance, the ratio fell from 1.5 to 0.3.

The Specific Resistance for Current Flow from the Cellular into the External Fluid Compartments R_z. The resistance R_z had to be determined from an analysis of voltage spread in the epithelial layer. In these experiments, two microelectrodes were used, one for passing current into an epithelial cell and a second one for exploring the electrical field in the neighboring cells. Hence, in addition to time and current strength, the location of the electrodes in the epithelial plane had to be considered as a further parameter.

Fig. 9 shows the time course of the voltage deflections which were observed with an intracellular microelectrode when square wave current pulses were passed into a nearby cell. Although the rising phase clearly depends on the distance between the current and the voltage cell, it can be

seen that the voltage in all cases eventually reaches a constant value. In contrast to the observations with transepithelial current flow (compare Fig. 7), no secondary voltage creep could be discerned in this case, even if the current flow was kept constant for 5 sec. The fact that the potential difference rises only slowly, when the distance between current and voltage cell is great, probably means that a greater number of cells has to be passed and that each cell acts as a R-C unit. From the results of Fig. 9 we conclude that the voltage deflections measured after approximately 1 sec (theoretically speaking at $t \to \infty$) can be used to determine the d-c resistance of the epithelial cells, provided that the interelectrode distance does not vastly exceed ~ 1 mm and that the applied currents are smaller or equal to the current used in this experiment (5.5×10^{-8} amps).

As can be seen in Fig. 10, currents of this magnitude already produced slight deviations from linearity in the current-voltage plot. With outward currents of 5.5×10^{-8} amps (current microelectrode-positive) the resistance calculated as $\Delta V_m/\Delta I$ appears to be $\sim 15\%$ smaller than the resistance measured with vanishing currents. With inward currents of the same magnitude the error is almost identical but in the opposite direction. The deviations did not show a clear dependence on the interelectrode distance. Despite these small deviations from linearity, the currents could not be reduced in the subsequent experiments in order to work in a strictly linear range because this would have hampered the accuracy of the voltage readings considerably.

Since the current might be expected to spread into all directions of the plane, the study of the voltage response as a function of electrode location must be described by two parameters. For example, if we place the origin of a system of polar coordinates above the current cell, we can move the voltage-recording electrode around, and can record ΔV_m as a function of interelectrode distance x and angle φ. Fig. 11 shows the results of such an experiment. It can be seen that the voltage attenuation was almost uniform in all directions. This observation is also supported by one experiment in which the voltage attenuation, measured at two different angles φ, was found to be almost undistinguishable (compare lines 4 and 5 in Table 1*a*). In one further experiment of this type, however, significant differences were noticed between the voltage attenuation at $\varphi = 0°$ and $\varphi = 90°$ (compare lines 2 and 3 in Table 1*a*). It is possible that this difference might have been caused by unequal stretch during mounting of the tissue. In contrast to toad urinary bladder [26] and *Necturus* stomach [7], where cell-to-cell coupling is restricted to single cell strains, no evidence for restricted coupling was found in gallbladder. Not a single cell out of ~ 200 cells

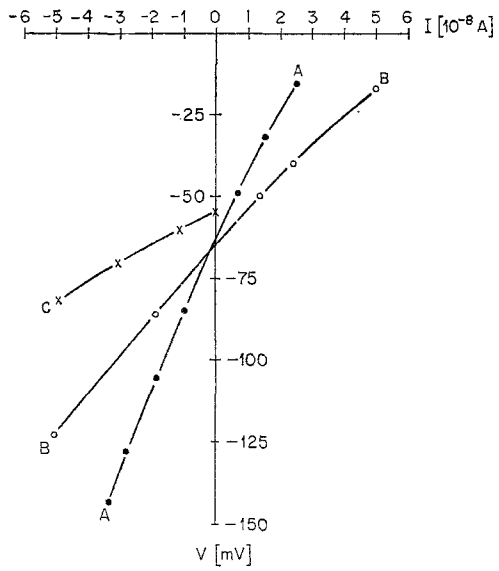

Fig. 10

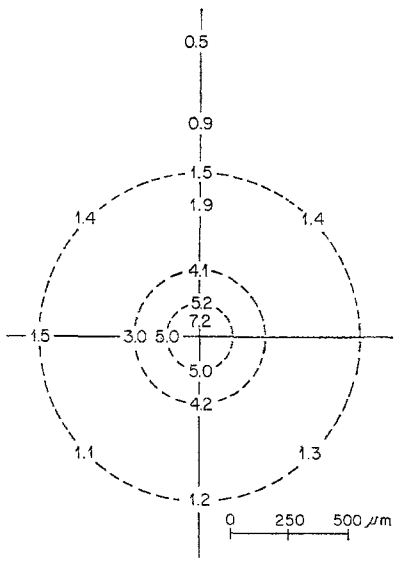

Fig. 11

Fig. 10. Current-voltage diagram for intracellularly applied current. *Abscissa:* current in 10^{-8} amps (outward current positive); *Ordinate:* cell membrane potential determined immediately before breaking the current pulse at 1.2 sec after onset of current. In experiment *A* the current and voltage electrode were situated in the same cell; in experiment *B* two immediately adjacent cells had been impaled; and in experiment *C* the cell-to-cell distance was 120 µm

Fig. 11. Voltage spread within the epithelial plane. The current cell was situated in the center of the coordinate system. The figures indicate the magnitude of the voltage deflections in mV, which were recorded from other cells situated at various distances and different angles from the current cells. The circles represent distances of 140, 280, and 660 µm from the current source

punctured in the current spread experiments failed to respond to the current pulse, provided that the distance between current and voltage cell was less than ~1 mm, and that the membrane potential in both cells was intact.

Fig. 12 finally gives an example of the voltage deflection ΔV_m as a function of distance. The data were obtained by moving electrode *B* at constant angle φ in radial direction from cell to cell. It can be seen that the experimental points fit well to the Bessel function, which has been derived from theoretical considerations in the Appendix. This result confirms that this analysis can predict the current spread in a plane sheet epithelium with uniform cell-to-cell coupling correctly. The same observation has also been made on intestinal mucosa [34]. In tubular epithelia, however, the intraepithelial voltage attenuation appears to follow a different pattern

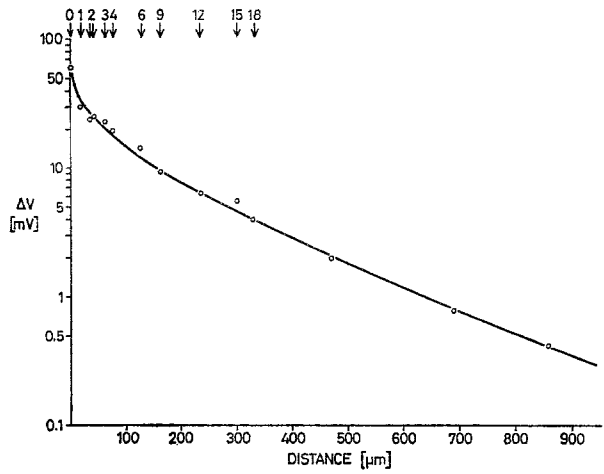

Fig. 12. Voltage attenuation as a function of radial distance. *Abscissa:* distance between voltage and current electrode; *Ordinate:* intracellular voltage deflections in mV in logarithmic scale. The open circles are the results from one experiment in which the current electrode was left within the current cell, while the voltage electrode was moved radially at constant angle φ to puncture different cells. As a result of the addition of sucrose to the interstitial bathing solution, the lateral spaces were dilated in this experiment and single cells could be clearly visualized and counted. The cell numbers are given in the top of the panel. No. 0 was the current cell. The sequence of impalements was: cells No. 6, 9, 12, 15, 18, 4, and 2. Then the three outermost points were obtained and the measurements were continued with cells No. 3, 2, 1, and 0. The results from individual cells were well reproducible. The curve depicts the Bessel function $\Delta V = 11.5\, K_0\left(\frac{x}{290}\right)$ (mV). It has been fitted to the results as described on pp. 272 and 273

since the experimental results from salivary glands of *Chironimous* [24, 26] and from kidney tubules [23, 44] show an exponential decay.

The Bessel function depicted in Fig. 12 has the following values of the constants: $A = 11.5$ mV and $\lambda = 290$ μm. From these values R_z is calculated for this particular gallbladder according to Eq. (A.12) to be 1,020 $\Omega\,\text{cm}^2$.

Simultaneous Determination of R_t, V_m/V_b, and R_z in Individual Gallbladders: In these experiments on six gallbladders, one or two series of current-spread measurements were made first to determine R_z. Immediately after they had been completed, current was passed transepithelially and the resistance R_t was determined as well as the ratio $\Delta V_m/\Delta V_b$ by puncturing several cells. The experimental results are compiled in Table 1 *a*. Columns 2 and 3 give the transepithelial resistance R_t which on the average was 307 $\Omega\,\text{cm}^2$ and the voltage divider ratio $\Delta V_m/\Delta V_b$ for which a mean value of 1.77 was obtained. The resistance for current flow from the cellular into the external fluid compartments R_z is given in column 4 and the resist-

Table 1 *a*. Experimental data for the determination of the paracellular shunt conductance according to Method I

Exp. no.	R_t (Ω cm^2)	$\frac{\Delta V_m}{\Delta V_b}$	R_z (Ω cm^2)	R_x (KΩ)	A (mV)	λ (μm)	Cellpd. (mV)	Direction of current	No. of cells
1	535	0.95	1,610	870	7.60	430	−44.0	out	12
2 a	295	2.36	3,490	780	6.80	670	−43.8	out	12
2 b	295	2.36	1,420	770	6.70	430	−48.3	out	12
3 a*	180	1.18	1,100	1,310	11.50	290	−47.5	out	14
3 b*	180	1.18	900	1,570	13.70	240	−51.6	out	11
4	345	1.05	2,140	380	3.33	750	−49.6	out	9
5	520	0.94	2,710	2,650	23.20	320	−41.7	in	12
6 a	300	2.32	700	380	3.33	430	−43.9	in	11
6 b*	115	3.62	920	500	4.36	430	−45.7	in	8
	307	1.77	1,666	1,023	8.94	443	−46.2		

* The measurements indicated by an asterisk have been performed in the presence of osmotically induced transepithelial water flow, after addition of 500 mmoles/liter sucrose to the serosal fluid.

Table 1 *b*. Results of the circuit analysis according to Method I[a]

Exp. No.	R_m (Ω cm^2)	R_b (Ω cm^2)	R_s (Ω cm^2)	$\frac{R_m + R_b}{R_s}$
1	3,140	3,300	583	11.1
2 a	11,730	4,970	300	55.6
2 b	4,770	2,020	308	22.0
3 a*	2,400	2,030	187	23.7
3 b*	1,960	1,660	189	19.2
4	4,390	4,180	359	23.8
5	5,260	5,590	546	19.9
6 a	2,320	1,000	329	10.1
6 b*	4,250	1,170	117	46.2
	4,470	2,880	324	25.7

[a] The values have been calculated from the data of Table 1 *a*.
* *See* Table 1 *a*.

ance for current flow from cell to cell R_x (*see* Appendix) in column 5. The latter two values have been calculated from the constants A and λ (columns 6 and 7) according to Eqs. (A.12) and (A.13). The last three columns contain information about the experimental conditions: the mean values of the cell membrane potentials, the direction of current flow (out: current microelectrode positive; in: current microelectrode negative) and the number of measurements in the individual experiments. Table 1 *b*

finally summarizes the results of the circuit analysis. The values have been calculated from the data in columns 2 through 4 of Table 1 *a* using Eqs. (5) through (8). The average resistance of the luminal cell membrane R_m turned out to be approximately 4,500 $\Omega\,cm^2$ and the lumped resistance of the basal cell membrane was approximately 2,900 $\Omega\,cm^2$. These values yield a total resistance of 7,400 $\Omega\,cm^2$, which has to be overcome, if current flows through the cells. Since the overall transepithelial resistance was only 307 $\Omega\,cm^2$, this result clearly demonstrates the existence of a highly conducting paracellular shunt path in *Necturus* gallbladder. For the resistance of the paracellular shunt path R_s a mean value of 324 $\Omega\,cm^2$ (column 4) was obtained. The mean ratio of the transcellular resistance *vs.* the paracellular resistance was 25, indicating that approximately 96% of the total current flows through the shunt path and only 4% flows through the cells.

Method II

Application of Method II required: 1) the determination of the voltage divider ratio $\Delta V_m/\Delta V_b$; 2) the determination of the resistance for current flow from the cell compartment into both external fluid compartments R_z; and 3) the determination of the resistance for current flow from the cellular into the interstitial fluid compartment with the luminal compartment being empty R_z'.

Since the voltage divider ratio had been determined in Method I, no further measurements were required. With respect to R_z, however, which had also been determined in Method I, it seemed preferable to obtain new measurements to minimize the influence of individual variations when comparing R_z to R_z'. Hence, an attempt was made to determine R_z and R_z' in the same gallbladders at the same place and at the same time. The following procedure was chosen: the current and voltage microelectrodes were positioned within different cells and the voltage deflections were recorded across the basal cell membrane while current flow was directed from the current cell either into the interstitial or into both external fluid compartments. Furthermore, the luminal fluid compartment was emptied and filled simultaneously as required. The data are listed in Table 2. They are expressed as $\Delta V_{b,\,i\to B}/\Delta V_{b,\,i\to A,B}$; that is the ratio of the voltage deflection observed during current flow into compartment B (with compartment A being empty) to the voltage deflection observed when the current was passed into compartments A plus B simultaneously. At cell-to-cell distances of 40 to 60 μm, the data yielded a mean ratio of 0.98 ± 0.21; at a distance of approximately 340 μm, the mean ratio was 0.90 ± 0.15; and at distances

Table 2. Ratio of the voltage deflections $r = \Delta V_{b,i\to B}/\Delta V_{b,i\to A,B}$ observed in the experiments of Method II as function of the distance x between current and voltage cell[a]

Group I		Group II		Group III	
x(μm)	r	x(μm)	r	x(μm)	r
60	0.88	340	0.72	680	1.00
40	0.86	360	1.07	600	1.07
35	1.22	340	0.83	640	0.95
35	0.75	340	0.97	600	1.06
60	1.19			530	0.96
			0.90	530	0.94
	0.98		±0.15		
	±0.21				1.00
					±0.06

[a] For derivation of the mean values, the data were split into three groups of short, medium and long cell-to-cell distance. Experiments in which the cell potential of the voltage or current cell had changed by more than 10% during emptying or filling of the luminal fluid compartment were discarded.

of 530 to 680 μm, the mean ratio was 1.00 ± 0.06. The fact that these ratios cannot be distinguished from unity, irrespective of the distance between the current and voltage cell, implies that R_z'/R_z is also close to unity. As has been discussed on p. 266 this result provides further independent evidence for the existence of a paracellular shunt path in *Necturus* gallbladder epithelium and indicates that the conductance of the shunt path ($1/R_s$) must be much higher than the conductance across the cell membranes ($1/R_m + R_b$). Because the data do not significantly deviate from unity[3], however, they do not allow a quantitative estimate of the shunt conductance to be obtained. Inserting the results from Method I into Eq. (12) (p. 266), the ratio R_z/R_z can be estimated to be 1.024. This value is not significantly different from the results in Table 2.

In the experiments of Table 2 the luminal fluid compartment was emptied when current was passed from the cell into the interstitium. This reduced the shunting effect of the surrounding epithelium for current flow from A to B and provided the basis for the application of Eq. (9) (p. 266). On the other hand, with the luminal fluid compartment remaining filled it was expected that the voltage attenuation would not depend on the direction of current flow since the shunt between A and B was now fully operative. This was indeed found. Under these conditions $\Delta V_{m,i\to B}/\Delta V_{m,i\to A,B}$ was 1.00 ± 0.05 and $\Delta V_{m,i\to A}/\Delta V_{m,i\to A,B}$ was 0.99 ± 0.04 (n = 12).

3 Even if the ratio of 0.90 from the experiments with cell-to-cell distances of 340 μm is taken as a real deviation and if a Bessel function is fitted through this point to determine R_z', no significant difference between R_z' and R_z is observed.

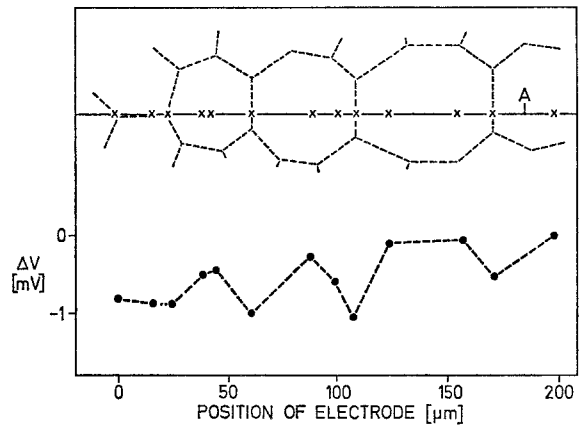

a

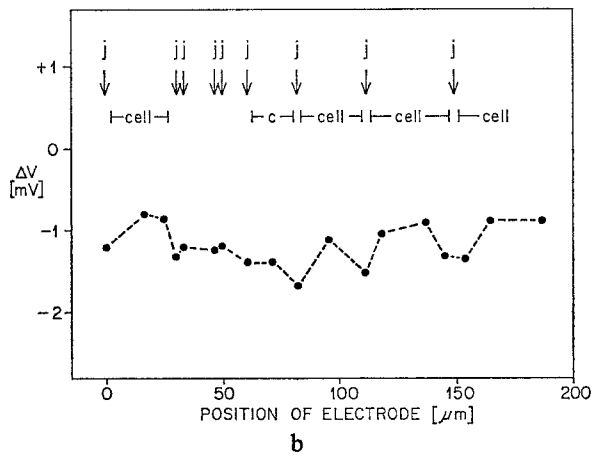

b

Fig. 13*a* and *b*. Voltage scan experiments. *Abscissa:* position of the electrode tip during its way across the luminal surface of the epithelium with respect to an arbitrary starting point in μm; *Ordinate:* current-induced potential difference in mV between the tip of the scanning electrode and a fixed point in the fluid bath nearby. Current density was 1.2 mamps/cm^2; direction of current flow was from lumen to interstitium. In the upper half of Fig. 13*a*, the approximate position of the cell borders is shown as visualized through the microscope. The solid line *A* indicates the path of the electrode. At every mark *x* the electrode movement was interrupted, and the potential difference was recorded. In Fig. 13*b* the position of the cells is indicated by bars (⊢ ⊣) and the position of the cell junctions *j* by the arrows (↓)

Voltage Scan Experiments

Although the experiments described above provided definite proof of the existence of a paracellular shunt, they did not specify the anatomical location. This question could be answered in further experiments in which current pulses were passed through the epithelium and a voltage scan of the mucosal surface of the gallbladdder was obtained. Fig. 13*a* and *b*

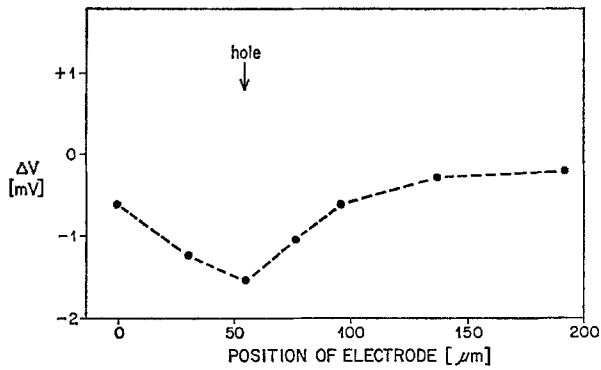

Fig. 14. Voltage scanning near a hole in the epithelial layer. *Abscissa* and *ordinate* as in Fig. 13. Direction of current flow was from lumen to interstitium, and current density was 0.18 mamp/cm^2. In this experiment a hole had been made in the epithelial layer, by poking a larger electrode through it. One cell was totally destroyed and immediately adjacent cells were injured. The path of the voltage scanning electrode led across the center of the hole, which is indicated by the arrow (↓)

give two examples of the results. It was observed that, whenever the tip of the field-exploring electrode was moved across a cell border, it indicated greater pulse deflections which were slightly more negative than when it was situated in the middle above a cell. Since the direction of current was lumen to interstitium (Fig. 3*a* and *b*), this result directly proves that the main part of the transepithelial current is funneled through the terminal bars into the lateral spaces and that the terminal bars are leaky and represent the paracellular shunt path.

The slight upward trend in the voltage curve of Fig. 13 is due to the fact that this particular experiment was made at the edge of a small blister which was formed by the epithelium after applying 2 to 4 cm of hydrostatic pressure to the serosal side. Thus, the electrode movement was not strictly horizontal in this measurement but slightly upwards along the wall of the blister. Under these conditions it was easier to keep the electrode tip during the backward movement in constantly close contact with the surface of the epithelium, since the epithelium could be slightly impressed with the electrode tip without damaging the cell membranes. The amount of hydrostatic pressure did not damage the tissue. It opened the lateral spaces and led to a decrease of the transepithelial resistance from 350 Ω cm^2 to 210 Ω cm^2, but the resistance rose to control values again when the pressure had been released.

The same technique of voltage scan was also used to look for other possible locations of a shunt and for possible edge damage effects. Since,

by simple inspection, no gaps could be recognized in the epithelial layer which might have been caused by cell desquamation during the regeneration process, the surface of the epithelium was explored randomly and special attention was paid to cells of slightly opaque appearance which were encountered sporadically. However, no evidence for regionally varying current densities was found. Furthermore, provided that the tissue was properly mounted and that protrusion of desquamated epithelium from underneath the edge of the chamber into the fluid bath was prevented, there was also no evidence for increased current flow through the edges. However, holes which had been made artificially by destroying one cell with a glass capillary, could be easily detected (Fig. 14).

Discussion

The present investigation has shown that a paracellular shunt path exists in *Necturus* gallbladder on which ions can bypass the cells on their way across the epithelium, that the conductance of the shunt path amounts to about 96% of the total conductance of the epithelium, and that the shunt path leads through the terminal bars or "tight junctions". These findings demonstrate that in gallbladder epithelium the "tight junctions" are really not tight for small ions in the direction of current flow from lumen to interstitium or back, and it would appear that the term "tight junction" should no longer be used in a general sense. However, before further consideration of the general implications of the present results, we want to discuss how the resistance of the paracellular shunt path and the coupling resistance between individual cells can be interpreted in terms of the histological structure of the gallbladder epithelium.

Does the Lateral Intercellular Space Contribute a Significant Amount to the Resistance of the Shunt Path across Necturus *Gallbladder?*

As shown in Fig. 1, the shunt path through the terminal bars (route No. 2 in Fig. 1) consists of two parts arranged in series: the terminal bar and the lateral intercellular space. Hence, in terms of the equivalent circuit of Fig. 2*a*, the resistance of the shunt path should be

$$R_s = R_j + n r_i \tag{15}$$

where nr_i is the unknown contribution of the lateral intercellular space and R_j the resistance of the terminal bars proper. By comparing the width of the lateral spaces obtained from electron-micrographs with conductance and

permeability data from rabbit and frog gallbladder, Smulders *et al.* [36] have recently shown that in these species the contribution of the lateral spaces to the gallbladder resistance is negligible under control conditions and becomes significant only during osmotically induced water flux from serosa to mucosa. This might be different in *Necturus* gallbladder, however. There are indeed three independent lines of evidence which suggest that the dimensions of the lateral spaces might have been of importance in our experiments.

1) Whereas Smulders *et al.* [36] have observed that the transepithelial resistance remained constant during water flux from mucosa to serosa, R_t decreased under these conditions in our experiments from control values of 200 to 500 $\Omega\,cm^2$ to values of about 110 to 180 $\Omega\,cm^2$. A similar fall of resistance was also observed during application of hydrostatic pressure to the serosal side of the epithelium or during current flow from mucosa to serosa. Since under all three measures the lateral spaces were seen to open, these observations would suggest that the resistance fall might have been caused predominantly by the dilatation of the lateral spaces, and that their contribution to the transepithelial resistance was not negligible.

2) The data of Table 1*a* suggest that there might be a negative correlation between R_t and $\Delta V_m/\Delta V_b$. This view is also supported by the observation that during osmotically induced water flux from serosa to mucosa the transepithelial resistance increased whereas the voltage divider ratio fell. A consistant negative correlation between these values could indicate that the lateral intercellular spaces play a significant role in our experiments, since R_t as well as R_b (and hence $\Delta V_m/\Delta V_b$) depend on r_i, the electrical resistance of the lateral spaces to current flow (compare Fig. 2*a* and *b*).

3) Finally, the approximate contribution of the lateral spaces to the transepithelial resistance can be calculated by considering the cell dimensions and assuming a range of space widths, according to:

$$R=\frac{\rho\ell}{F} \tag{16}$$

where R is the resistance in Ω, $\rho(\Omega\times cm)$ is the specific resistivity of the conducting material and $\ell(cm)$ and $F(cm^2)$ are the length (in direction of current flow) and the area of the body of the conducting material, respectively. Since we consider current flow in the transepithelial direction, ℓ must be identical to the cell height of about 30 μm (obtained from normal histology) and F can be calculated from the space width and from the total length of the network of lateral spaces contained in 1 cm^2 of epithelium. If we con-

sider the cells to be hexagonal and to have an average diameter of approximately 20 μm (compare Fig. 12) the network of lateral spaces within 1 cm^2 of epithelium should be 1,150 cm long. Since the specific resistivity of the fluid should be similar to that of Ringer's fluid ($\sim$100 Ω cm) the following resistances can be calculated. They are expressed per cm^2 of epithelial surface. At a space width of 1 μm the contribution of the lateral spaces to the total transepithelial resistance should be only 2.6 Ω. At a width of 0.1 μm it should be 26 Ω and at 0.01 μm, 260 Ω. The latter value, however, might actually be considerably higher, since at small space widths the tortuosity of the channels should be taken into account, which is especially pronounced in *Necturus* gallbladder (H. Pockrandt-Hemstedt, *personal communication*).

From these data it would appear that under conditions of maximal dilatation as for example during osmotically induced water flux from mucosa to serosa the resistance of the lateral spaces is negligible in *Necturus* gallbladder, and that the transepithelial resistance of 110 to 180 Ω cm^2 measured under these conditions is for all practical purposes identical with the resistance of the junctional complexes alone. At space widths below 0.1 μm, however, the resistance of the intercellular spaces can no longer be neglected. To explain the difference between the value of 110 to 180 Ω cm^2 and the actual transepithelial resistances, which we have observed under control conditions, the spaces should have had a width of approximately 0.01 to 0.03 μm or 100 to 300 Å; and if tortuosity is considered, the space width might have been in the range of 300 to 1,000 Å. This range does not seem unlikely in view of the electron-microscopic observations of Tormey and Diamond [39] and Smulders *et al.* [36] in rabbit gallbladder, but a final statement has to wait until similar studies in *Necturus* gallbladder are available.

Quantitative Aspects of Current Flow through The Terminal Bars in Relation to Electron-microscopic Findings

The electron-microscopic structure of the terminal bars has already been described quite extensively. A terminal bar consists of two parts, a *zonula occludens*, which faces the luminal fluid compartment and a *zonula adherens*, which faces the lateral intercellular space. Both surround the edge of the cells completely like belts. In gallbladder epithelium of guinea pig [17], rabbit [39] and *Necturus* (J. M. Tormey, *personal communications*) the *zonula occludens* is approximately 2,000 Å deep. It consists of a very close apposition of the two plasma membranes of the adjacent cells. Previously, it was thought that the two outer leaflets of the plasma membrane were fused over the entire depth of the zonula occludens. However, recent observations have

shown that the two plasma membranes form only a number of punctate contacts, whereas for the major part of the zonula, the two membranes are clearly separated and leave spindlelike open spaces between them [22, 39]. In freeze-cleave studies on similar junctions in intestinal [37] and liver cells [22] the contact points appear to be formed of threads or chains of small globular particles which connect the two apposing membrane phases and leave a labyrinth of tortuous, probably aqueous channels between them.

The depth of the *zonula adherens* is more variable in gallbladder epithelium [17] but generally in the same order of magnitude as the depth of the zonula occludens. In the zonula adherens, the plasma membranes are clearly separated over the entire length by a cleft of constant width of about 200 Å, which contains material of relatively low electron density.

The electron-microscopic studies have also shown that the main resistance for the transepithelial exchange of matter is not located in the zonula adherens but rather in the zonula occludens. Thus, it has been observed that large protein molecules, as well as ferritin and colloidal lanthanum, when applied from the interstitial surface of the epithelium, can easily penetrate into the cleft of the zonula adherens but cannot penetrate into the zonula occludens [17, 22, 28, 38]. The latter is also true when the substances are applied from the luminal surface.

Since our experiments have shown that electric current in contrast can pass the terminal bars easily one can envisage the function of the zonula occludens as follows: The threads or chains of globular particles may act as weirs and provide the barrier for the transepithelial movement of larger particles and protein molecules. Ions and smaller molecules however, may penetrate relatively easily through small gaps between the globular particles. They may then reach the network of aqueous channels which extends throughout the entire depths of the zonula occludens and proceed their path along these channels until they arrive at the next weir. Thus, the greater part of the transport along the zonula occludens could be governed by mechanisms similar to those in simple aqueous solutions, and there would be only a few, possibly only two occasions (if the channels within the zonula were continuous from one end to the other), where the ions could interact stronger with the membrane, namely during the passage through the weirs. Although this view might seem highly speculative it appears to be compatible with the following calculations of specific resistivities which can be derived from the present results.

As we have discussed above, the resistance of the network of terminal bars of 1 cm^2 of gallbladder epithelium for transepithelial current is approximately 110 to 180 $\Omega\,cm^2$. This value represents the sum of the resistances

of the zonula adherens and of the zonula occludens. For the resistance of the zonula adherens, a relatively safe estimate can be obtained under the assumption that the resistivity of the fluid within the cleft is approximately equal to that of Ringer's fluid. Since the total length of the network of terminal bars within 1 cm^2 of epithelium is about 1,150 cm (*see* p. 289) and since the cleft is about 200 Å $= 2 \times 10^{-6}$ cm wide and measures about 2,000 Å $= 2 \times 10^{-5}$ cm in the direction of current flow, the resistance of the zonula adherens should be a little less than 1 Ω per cm^2 of epithelium, as can be calculated from Eq. (16) (p. 288). This result allows the conclusion that the resistance of the zonula adherens is negligible compared to that of the zonula occludens; and this conclusion would even hold if the resistivity of the fluid within the cleft were one order of magnitude higher than that of Ringer's fluid.

If we now consider the dimensions of the zonula occludens and assume that the width of the aqueous channels is between 20 and 70 Å, we can calculate from Eq. (16) that the specific resistivity of the fluid within these channels must range between ca. 1,700 and 6,000 Ω cm. These values are considerably greater than the resistivity of Ringer's fluid and thus allow for greater restriction of ion movement in the regions of chainlike structures as well as for membrane ion interaction at the walls of the channels and for tortuosity of the channels.

The Route of Current Flow from Cell to Cell

Although we have seen that transepithelial current passes almost entirely through the terminal bars, the route of current flow from cell to cell is not precisely known. Among the various types of junctions between electrically coupled cells which have been described by electron-microscopists it is most likely that the so-called nexus or gap junctions are electrically conducting. These junctions have been observed in heart [4, 12, 29] and smooth muscle [12], and in several electrically coupled epithelia such as liver [22], cervix uteri [29] and renal proximal tubules [35]. Aside from these, a special type of "focal tight junctions" appears to be conducting in chicken embryo [40] and septate desmosomes are thought to provide electrical coupling in invertebrate tissue [9]. Since recent electron-microscopic studies on *Necturus* gallbladder have indicated that gap junctions do also occur in gallbladder epithelium (H. Pockrandt-Hemstedt, *personal communication*), it would seem likely that cell-to-cell coupling is also mediated via gap junctions in *Necturus* gallbladder.

On the other hand, however, the possibility remains that other cell membrane junctions contribute a significant amount to horizontal current

flow. Desmosomes are not likely to conduct current from cell to cell since they do occur between electrically uncoupled nerve cells and do not participate in electrical transmission in heart muscle [15]. This is in agreement with their electron-microscopic appearance which shows a wide cleft between the adjacent cell membranes. The latter is also true for the zonula adherens. A contribution of the zonula occludens to current flow from cell to cell, however, cannot be ruled out at present. If current could flow across the zonula occludens in the horizontal direction we would have to postulate that this route of current flow be highly insulated against the transepithelial route to explain our observation of cell-to-cell coupling in the presence of a low-resistance paracellular shunt through the junctions in the transepithelial direction. Evidence for a good insulation of the cell interior against the extracellular fluid at the junctional level has also been obtained in other tissues by both electrical and tracer experiments [25]. Thus, in case of a significant contribution of the zonula occludens to horizontal current flow, the following submicroscopic picture of the junctions could be envisaged: The globular particles which form the fusion sites between the apposing cell membranes might have some kind of central "bore" through which ions and small molecules might pass from cell to cell without coming in contact with the surrounding, probably aqueous channels within the zonula occludens which carry out the transport in the transepithelial direction.

Significance of the Results in View of Transport Mechanisms

Since the occurrence of terminal bars with a distinct zonula occludens is a general feature of epithelia, the question arises as to what extent our findings in gallbladder can be generalized. Are terminal bars leaky in all epithelia or do some epithelia exist in which the terminal bars are tight? This question cannot be answered precisely at present since, aside from the data from renal proximal tubules and from gastric mucosa which have been cited in the Introduction, only indirect evidence is available. However, a careful evaluation of the available indirect evidence in terms of different criteria derived by Barry *et al.* [5], has led us to the conclusion that besides gallbladder and renal proximal tubules the small intestine and the choroid plexus may have very leaky junctions and that the conductance through the junctions may be comparable to or smaller than the conductance through cells – but not necessarily negligible – in gastric mucosa, frog skin, toad urinary bladder and salivary ducts. (For details *see* ref. [19].) In view of this result it would appear that the importance of paracellular transport routes should no longer be neglected *a priori* in any epithelium and that in describing

any transport parameters an attempt should be made to separate the relative contributions of the cellular and paracellular pathways. This is especially important when models of the transport mechanisms are considered.

One example which illustrates this point is the model of isotonic fluid transport in gallbladder as proposed by Diamond and Bossert [14]. Since pertinent information was not available at that time, the authors assumed that the terminal bars were tight and that all water and all ions flowed through the cell membranes. However, there are at least two observations which support the view that the tight junctions may also have a significant permeability to water: 1) The present experiments show that the transepithelial route through the zonula occludens has a very low electrical resistivity compared to that of other membrane material. 2) The channels for passive ion movement through the gallbladder epithelium (which have been shown in this paper to be located in the zonula occludens) lack marked ion selectivity [5]. Both observations point to a highly hydrated membrane, and a highly hydrated membrane is also likely to exhibit a high water permeability. In view of this reasoning it would seem necessary to consider a modification of the model of isotonic water transport in which solutes and water would also be able to flow from the luminal fluid compartment through the terminal bars into the lateral space.

Such a modified model can be conceived to work as follows: As the first step, sodium ions and bicarbonate or chloride are actively transported from the lumen through the cell into the lateral intercellular space. Thus, a local osmotic gradient is built up between the lateral space and the luminal fluid compartment. This gradient causes osmotic water flow from the lumen into the lateral space via two different routes: via the terminal bars and via the cellular compartment. The interesting property of the first route is that, depending on the reflection coefficient of the terminal bars for NaCl, besides water, salt should also be transferred from the lumen into the lateral space by a mechanism of solvent drag, whereas the second route may serve for the fine adjustment of the transported fluid to isotonicity, which seems to occur at the basal end of the lateral space. The fluid transport from the lateral spaces across the basement membrane into the interstitium then is essentially a hydrodynamic flow governed by hydrostatic and oncotic forces.

This model has several aspects in common with different model assumptions, which have already been discussed in the literature [11, 18, 32] and would seem to apply not only to gallbladder but also to proximal tubules of mammalian kidney [3] and to human jejunum [18]. It has the following interesting aspects: 1) It demonstrates that the reflection coefficient for NaCl is a very important property of the membrane which, especially in epithelia,

should be determined in any case. 2) It can easily explain our observation that the active sodium transport through an epithelium can be "amplified" by a superposition of a passive sodium transport component. This situation occurs in proximal tubules of the rat kidney, where only approximately one-half of the net sodium transport appears to be active, while the other half has to be considered as passive [3].

Appendix

Analysis of Intraepithelial Voltage Spread: Determination of R_z

The problem of current spread around a point source in a flat conducting sheet has already been discussed in the literature [16, 31, 34, 45]. However, the two reports [16, 34] which give a complete analysis of the problem, regard the two fluid compartments, which the plane sheet faces on either side, as being always at the same potential. In the present study, in contrast, the two fluid compartments are considered separately. This requires a slightly different formulation of the problem, which will be outlined in the following.

On p. 263 we have presented a basic equivalent circuit which represents a single cell with a paracellular shunt path and which consists of the three lumped resistors R_m, R_b and R_s (Fig. 2*b*). This basic circuit describes the electric response of a cell properly if the voltage response of all neighboring cells is identical. This situation obtains during the determination of the transepithelial resistance R_t and during determination of the voltage divider ratio $\Delta V_m/\Delta V_b$. However, when the voltage response of individual cells differs, as for example when current is injected only into one cell and spreads horizontally within the entire cell layer, we have to consider the entire two-dimensional assembly of cells simultaneously. This can be done by help of the network depicted in Fig. 15*a* which is thought to consist of an infinite number of electrically coupled single cells. The cells are represented by the basic circuit diagram of Fig. 2*b*, consisting of the resistance of the luminal cell membrane r_m, of the basal cell membrane r_b and of a paracellular shunt path r_s. C_1, C_2 and C_3 are the intracellular fluid compartments of 3 neighboring cells which are connected by coupling resistors r_x. A and B represent the luminal and interstitial fluid compartment, r_{fa} and r_{fb} are the resistances for current flow in these compartments. Usually, they can be neglected.

This circuit diagram can be simplified if compartments A and B are shorted. By shorting r_s, lumping r_m and r_b into r_z and folding the circuit within line $C_1 \ldots C_n$ we obtain the simple cable-like network depicted in Fig. 15*b*.

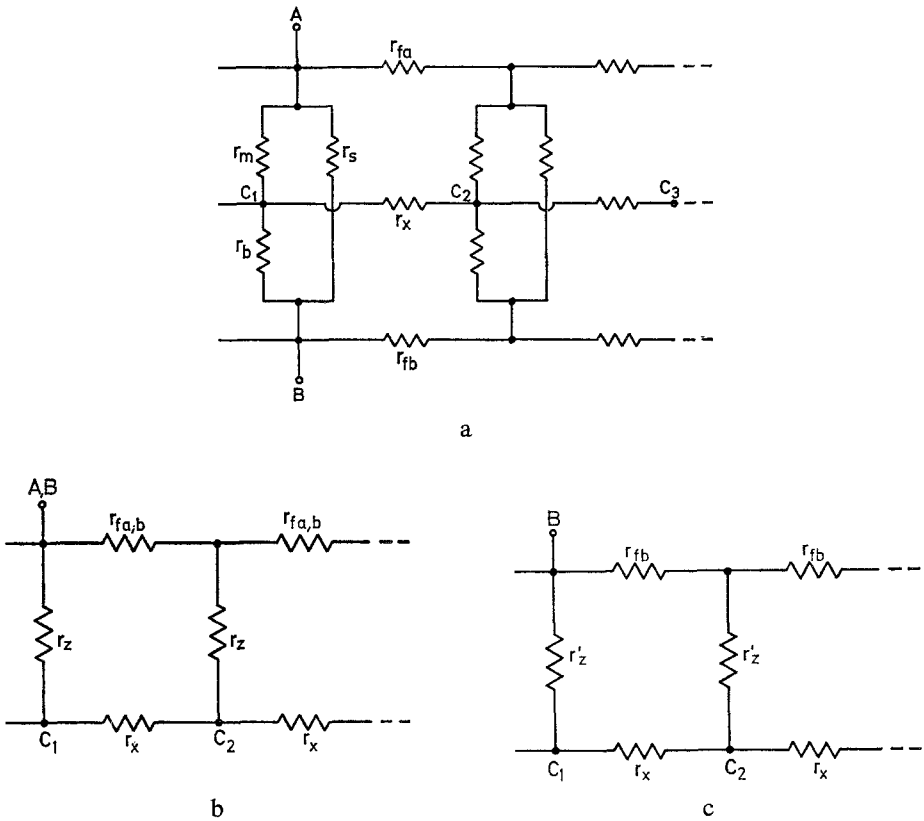

Fig. 15*a*, *b* and *c*. Network of electrically coupled epithelial cells. *A:* Individual cells are represented by the basic equivalent circuit of Fig. 3. Adjacent cells are interconnected at their *C*-terminals, which represent the cellular fluid compartments, through coupling resistors r_x. (For details *see* text). *B* and *C:* Reduced forms of the same network which have been used to describe the experiments of Methods I and II, respectively

In this circuit, r_z is given by

$$\frac{1}{r_z}=\frac{1}{r_m}+\frac{1}{r_b}. \tag{A.1}$$

This approach was used in the experiments of Method I. Experimentally, the shortcircuit between *A* and *B* can be achieved by providing two different current electrodes and placing them into compartments *A* and *B* simultaneously. On the other hand, however, it should be noticed that the epithelium itself already provides a shortcircuiting element between compartments *A* and *B* during the determination of R_z. To explain this we will consider a situation in which current is passed from a cell into compartment *A* with compartment *B* floating, and we will assume for the sake of simplicity that R_s is infinite. If only one cell is exposed between chambers *A* and *B*,

or if current is passed at equal densities into all exposed cells simultaneously, there will be no shunt. All current will pass from C to A via r_m and there will be no current flow via r_b. However, if more cells are exposed, and if current is injected only into one cell C_1 the situation is different. Current will now flow along the chain of cells $C_1 \ldots C_n$ and cross the resistors $r_{m1} \ldots r_{mn}$ to reach compartment A, and, in addition, some current will also flow across the resistors r_b into compartment B. This is possible since the remote cells C_m which are not reached by the intracellularly propagating current will now act as a shunt between A and B so that the current leaving $C_1 \ldots C_n$ via $r_{b1} \ldots r_{bn}$ can flow along the resistors r_{fb} and pass through the remote cells C_m from B into A. The efficiency of this shunt depends on the conductance of the external fluid compartments for horizontal current and on the ratio of the space constant to the area of epithelium which is exposed between chambers A and B.

Another possible choice to simplify the circuit diagram of Fig. 15*a* is to make r_{fa} infinite; that is, to interrupt the horizontal conductance within the luminal fluid compartment, represented by line A in Fig. 15*a*. This operation reduces the circuit again to a cable-like network as depicted in Fig. 15*c*. Instead of r_z, however, we are now dealing with a different resistor r_z' which represents r_m, r_b and r_s according to

$$\frac{1}{r_z'} = \frac{1}{r_b} + \frac{1}{r_m + r_s}. \tag{A.2}$$

Experimentally, the latter situation can be approached by emptying the luminal fluid compartment, so that a thin fluid film remains at the luminal surface. The current will then be able to pass from the cell across the luminal cell membrane into the film and it will return through the nearest shunt path into the interstitial fluid compartment B if the film is thin so that current spread in the horizontal direction (along line A in Fig. 15*a*) is reduced. This approach was used in the experiments of Method II.

Fig. 15*a,b* and *c* have to be considered as a planar array of resistors rather than as a single transmission line. To derive the voltage as a function of cell-to-cell distance in such a two-dimensional array we regard the homogeneous model depicted in Fig. 16. In this model all resistive elements r_x which allow current flow in the horizontal direction are distributed into a uniform thin plane sheet of infinite extension C. This plane sheet is thought to be connected on one side through a membrane M to a reservoir of infinite conductivity A, assuming $r_{fa,b}$ and r_{fb} in Fig. 15*b* and *c* to be zero. Into membrane M all resistive elements r_z are lumped which allow current flow in the perpendicular direction, from C to A in Fig. 16. If the conducting

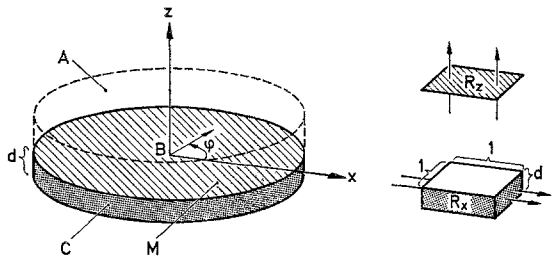

Fig. 16. Diagram to illustrate the mathematical treatment of current spread within a plane. (For details *see* text).

material of the plane sheet C has a specific resistivity ρ and a thickness d, the resistance for current flow in the horizontal direction of 1 cm^2 of the sheet will be $R_x = \frac{\rho}{d}$ (Ω). The specific resistance of membrane M for current flow in the z-direction is R_z(Ω cm^2). In the center B of the plane sheet a point source of electric current is located at $x=0$ and $z=0$. Current can flow radially within sheet C and cross the membrane M on its way to the reservoir A. The thickness d of the conducting sheet C is considered to be so small that current flow within the sheet is not a function of z.†

Now let us consider an infinitesimal cylindrical element of the conducting sheet of inner radius x and outer radius $x+dx$. The infinitesimal resistance dr_x for current flow in the radial direction (x-direction) through this element is

$$dr_x = \frac{R_x}{2\pi x} dx \tag{A.3a}$$

and the infinitesimal conductance $d\sigma_x$ for current flow in the z-direction through membrane M is

$$d\sigma_x = \frac{2\pi x}{R_z} dx. \tag{A.3b}$$

Furthermore, the decrement of the voltage dV across membrane M between a point x and a point $x+dx$ is given by

$$dV = I_x(x)\, dr_x. \tag{A.4a}$$

Since the decrement of the radial current dI_x within sheet C equals the infinitesimal current through membrane M, we obtain

$$dI_x = j_z(x)\, 2\pi x\, dx = V(x)\, d\sigma_x \tag{A.4b}$$

where j_z is the current density through membrane M.

† This simplification is justified as long as we consider only regions of $x > d$. For a complete analysis of the voltage spread in case $x < d$ *see* ref. [16].

Inserting Eqs. (A.3a) and (A.3b) into Eqs. (A.4a) and (A.4b) leads to

$$\frac{dV}{dx}=I_x(x)\frac{R_x}{2\pi x} \tag{A.5a}$$

and

$$\frac{dI_x}{dx}=V(x)\frac{2\pi x}{R_z}. \tag{A.5b}$$

After differentiation of Eq. (A.5a) and insertion of Eqs. (A.5a) and (A.5b) we obtain a Bessel differential equation with imaginary argument and $n=0$.

$$\frac{d^2V}{dx^2}+\frac{1}{x}\frac{dV}{dx}-\frac{V}{\lambda^2}=0 \tag{A.6}$$

where λ has been defined as

$$\lambda\equiv\sqrt{R_z/R_x}. \tag{A.7}$$

The general solution of Eq. (A.6) is

$$V=AK_0\left(\frac{x}{\lambda}\right)+BI_0\left(\frac{x}{\lambda}\right) \tag{A.8}$$

where K_0 and I_0 are zero order modified Bessel functions. Since under our boundary conditions V will become zero for $\frac{x}{\lambda}\to\infty$, B must be zero. The solution then reads

$$V=AK_0\left(\frac{x}{\lambda}\right). \tag{A.9}$$

The meaning of constant A can be understood when the current flow is considered through membrane M. From Eq. (A.4b) we obtain

$$j_z(x)2\pi x\,dx=AK_0\left(\frac{x}{\lambda}\right)\frac{2\pi x}{R_z}dx. \tag{A.10}$$

After integrating from $x=0$ to $x=\infty$ this equation yields

$$i_0=\frac{2\pi A\lambda^2}{R_z}\int_0^\infty\left(\frac{x}{\lambda}\right)K_0\left(\frac{x}{\lambda}\right)d\left(\frac{x}{\lambda}\right) \tag{A.11}$$

with i_0 being the total current applied. Since the value of the integral is equal to 1 [1] we obtain the relations

$$R_z=\frac{2\pi A\lambda^2}{i_0} \tag{A.12}$$

and

$$R_x=\frac{\rho}{d}=\frac{2\pi A}{i_0}. \tag{A.13}$$

Hence, to determine the values of R_z and R_x, the total current and the constants A and λ have to be known. The constants can be obtained by fitting the appropriate Bessel function to the experimentally determined voltage attenuation as a function of radial distance x.

I would like to thank Dr. J. M. Diamond for having arranged my stay at his laboratory and for many helpful discussions with regard to the experimental work and to the publication. My thanks are also due to Drs. J. Bereiter-Hahn, R. S. Eisenberg, W. New, W. S. Rau, J. M. Tormey, K. J. Ullrich, E. M. Wright, and Mr. M. Kübel for various comments and to Miss K. Lüer for perfect technical assistance.

References

1. Abramowitz, M., Stegun, I. A. 1965. Handbook of Mathematical Functions. National Bureau of Standards, Washington, D. C. Fourth printing. p. 486.
2. Adrian, R. H. 1956. The effect of internal and external potassium concentration on the membrane potential of frog muscle. *J. Physiol.* **133**:631.
3. Baldamus, C. A., Frömter, E., Lüer, K., Radtke, H. W., Rumrich, G., Sauer, F., Ullrich, K. J. 1972. Transport parameters for sodium, chloride and bicarbonate in proximal tubules of the rat kidney. (In preparation).
4. Barr, L., Dewey, M. M., Berger, W. 1965. Propagation of action potentials and the structure of the nexus in cardiac muscle. *J. Gen. Physiol.* **48**:797
5. Barry, P. H., Diamond, J. M., Wright, E. M. 1971. The mechanism of cation permeation in rabbit gallbladder. Dilution potentials and biionic potentials. *J. Membrane Biol.* **4**:358.
6. Bentzel, C. J., Parsa, B., Hare, D. K. 1969. Osmotic flow across proximal tubule of *Necturus:* Correlation of physiologic and anatomic studies. *Amer. J. Physiol.* **217**:570.
7. Blum, A. L., Hirschowitz, B. I., Helander, H. F., Sachs, G. 1971. Electrical properties of isolated cells of *Necturus* gastric mucosa. *Biochim. Biophys. Acta* **241**:261.
8. Boulpaep, E. 1971. Electrophysiological properties of the proximal tubule: Importance of cellular and intercellular pathways. *In*: Electrophysiology of Epithelia. G. Giebisch, editor. p. 91. K. Schattauer Verlag, Stuttgart.
9. Bullivant, S., Loewenstein, W. R. 1968. Structure of coupled and uncoupled cell junctions. *J. Cell Biol.* **37**:621.
10. Clarkson, T. W. 1967. The transport of salt and water across isolated rat ileum. Evidence for at least two distinct pathways. *J. Gen. Physiol.* **50**:695.
11. Curran, P. F., MacIntosh, J. R. 1962. A model system for biological water transport. *Nature* **193**:347.
12. Dewey, M. M., Barr, L. 1964. A study of the structure and distribution of the nexus. *J. Cell. Biol.* **23**:553.
13. Diamond, J. M. 1962. The mechanism of solute transport by the gallbladder. *J. Physiol.* **161**:474.
14. Diamond, J. M., Bossert, W. H. 1967. Standing-gradient osmotic flow. A mechanism of coupling of water and solute transport in epithelia. *J. Gen. Physiol.* **50**:2061.
15. Dreifuss, J. J., Girardier, L., Forssmann, W. G. 1966. Étude de la propagation de l'excitation dans le ventricule de rat au moyen de solutions hypertoniques. *Pflüg. Arch. Ges.Physiol.* **292**:13.
16. Eisenberg, R. S., Johnson, E. A. 1970. Three-dimensional electrical field problems in physiology. *Prog. Biophys. Mol. Biol.* **20**:1.
17. Farquhar, M. G., Palade, G. E. 1963. Junctional complexes in various epithelia. *J. Cell. Biol.* **17**:375.

18. Fordtran, J. S., Rector, F. C., Jr., Carter, N. W. 1968. The mechanism of sodium absorption in the human small intestine. *J. Clin. Invest.* **47**:884.
19. Frömter, E., Diamond, J. M. 1972. Route of passive ion permeation in epithelia. *Nature New Biol.* **235**:9.
20. Frömter, E., Müller, C. W., Wick, T. 1971. Permeability properties of the proximal tubular epithelium of the rat kidney studied with electrophysiological methods. *In:* Electrophysiology of Epithelia. G. Giebisch, editor. p. 119. K. Schattauer Verlag, Stuttgart.
21. Giebisch, G. 1958. Electrical potential measurements on single nephrons of *Necturus*. *J. Cell Comp. Physiol.* **51**:222.
22. Goodenough, D. A., Revel, J. P. 1970. A fine structural analysis of intercellular junctions in the mouse liver. *J. Cell Biol.* **45**:272.
23. Hoshi, T., Sakai, F. 1967. A comparison of the electrical resistances of the surface cell membrane and cellular wall in the proximal tubule of the *Newt* kidney. *Jap. J. Physiol.* **17**:627.
24. Loewenstein, W. R. 1966. Permeability of membrane junctions. *Ann. N.Y. Acad. Sci.* **137**, Pt. 2:441.
25. Loewenstein, W. R., Kanno, Y. 1964. Studies on an epithelial (gland) cell junction. *J. Cell. Biol.* **22**:565.
26. Loewenstein, W. R., Socolar, S. J., Higashino, S., Kanno, Y., Davidson, N. 1965. Intercellular communication: renal, urinary bladder, sensory, and salivary gland cells. *Science* **149**:295.
27. Lundberg, A. 1957. The mechanism of establishment of secretory potentials in sublingual gland cells. *Acta Physiol. Scand.* **40**:35.
28. Maunsbach, A. 1966. Absorption of ferritin by rat kidney proximal tubule cells. *J. Ultrastruct. Res.* **16**:1.
29. McNutt, N. S., Weinstein, R. S. 1970. The ultrastructure of the *Nexus*. *J. Cell Biol.* **47**:666.
30. Nastuk, W. L., Hodgkin, A. L. 1950. Electrical activity of single muscle fibers. *J. Cell Comp. Physiol.* **35**:39.
31. Noble, D. 1962. The voltage and time dependence of the cardiac membrane conductance. *Biophys. J.* **2**:381.
32. Patlak, C. S., Goldstein, D. A., Hoffman, J. F. The flow of solute across a two-membrane system. *J. Theoret. Biol.* **5**:426.
33. Sakai, F., Hoshi, T., Haga, M., Enomoto, Y. 1961. Membranpotential der Nierentubuli des Triturus Pyrrhogaster. *Jap. J. Pharmacol.* **11**:65.
34. Shiba, H. 1971. Haevisides "Bessel cable" as an electric model for flat simple epithelial cells with low resistive junctional membranes. *J. Theoret. Biol.* **30**:59.
35. Silverblatt, F. S., Bulger, R. E. 1970. Gap junctions occur in vertebrate renal proximal tubule cells. *J. Cell Biol.* **47**:513.
36. Smulders, A., Tormey, J. M., Wright, E. M. 1972. The effect of osmotically induced water flows on the permeability and ultrastructure of the rabbit gallbladder. *J. Membrane Biol.* **7**:164.
37. Staehelin, L. A., Mukherjee, T. M., Williams, A. W. 1969. Freeze etch appearance of the tight junctions in the epithelium of small and large intestine of mice. *Protoplasma* **67**:165.
38. Thoenes, W., Langer, K. H. 1969. Die Endozytosephase der Eiweißresorption im proximalen Nierentubulus. *Virchows Arch. Abt. B Zellpath.* **2**:361.
39. Tormey, J. M., Diamond, J. M. 1967. The ultrastructural route of fluid transport in rabbit gallbladder. *J. Gen. Physiol.* **50**:2031.
40. Trelstad, R. L., Revel, J. P., Hay, E. D. 1966. Tight junctions between cells in the early chick embryo as visualized with the electronmicroscope. *J. Cell Biol.* **31**:C6.

41. Ussing, H. H., Windhager, E. E. 1964. Nature of shunt path and active sodium transport path through frog skin epithelium. *Acta Physiol. Scand.* **61**:484.
42. Wedner, H. J., Diamond, J. M. 1969. Contributions of unstirred-layer effects to apparent electrokinetic phenomena in gallbladder. *J. Membrane Biol.* **1**:92.
43. Wick, T., Frömter, E. 1967. Das Zellpotential des proximalen Konvoluts der Rattenniere in Abhängigkeit von der peritubulären Ionenkonzentration. *Pflüg. Arch. Ges. Physiol.* **294**:R 17.
44. Windhager, E. E., Boulpaep, E. L., Giebisch, G. 1967. Electrophysiological studies on single nephrons. *Proc. 3rd. Int. Congr. Nephrol.*, Washington (1966), vol. 1, p. 35. Karger Basel, New York.
45. Woodburry, J. W., Crill, W. E. 1961. On the problem of impulse conduction in the atrium. *In:* Nervous Inhibition, E. Florey. editor. p. 124. Pergamon Press, N.Y.
46. Wright, E. M., Barry, P. H., Diamond, J. M. 1971. The mechanism of cation permeation in rabbit gallbladder. Conductances, the current-voltage relation, the concentration dependence of anion-cation discrimination, and the calcium competition effect. *J. Membrane Biol.* **4**:331.
47. Wright, E. M., Diamond, J. M. 1968. Effects of pH and polyvalent cations on the selective permeability of gallbladder epithelium to monovalent ions. *Biochim. Biophys. Acta* **163**:57.